Bulgarian Chemical Communications, Volume 48, Special Issue E (pp. 384 - 390) 2016

Protective multilayer (Ti, Al) N coatings deposited at low temperature by closed-field unbalanced magnetron sputtering

T. M. Cholakova[1*], V. A. Chitanov[1], L. P. Kolaklieva[1], R. D. Kakanakov[1], D.G. Kovacheva[2], P. K. Stefanov[2], S. N. Rabadzhiyska[1], E. A. Korina[1], V. I. Kopanov[1]

[1]*Central Laboratory of Applied Physics, Bulgarian Academy of Sciences, 61 Sankt Petersburg Blvd., 4000 Plovdiv, Bulgaria*

[2] *Institute of General and Inorganic Chemistry, Bulgarian Academy of Sciences, 1113 Sofia, Bulgaria.*

This article reports the results of a study of the physical-mechanical properties of the multilayer Ti-Al-N coatings deposited onto two types of substrates: high-speed steel and carbon tool steel. The coatings were deposited at the temperatures of 150-200 ºC by closed-field reactive unbalanced magnetron sputtering, while the process parameters were optimized to achieve adherent good quality coatings. Nanoindentation, scratch tests, X-ray diffractometry (XRD) and X-ray photoelectron spectroscopy (XPS) were used to characterize structural, compositional and mechanical properties of the coatings. The obtained coatings exhibited nanohardness and elastic modulus in the range of 26-38 GPa and 320-418 GPa respectively. The results of the scratch tests showed that the state of adhesion of the coating to the substrate depends on the coating deposition conditions. The measured coefficient of friction for all of the coatings was in the range of 0,09-0,13. The XPS and XRD analyses revealed that the coatings have $Ti_{0.42}Al_{0.58}N$ composition with a lattice constant of 4.17Å. The findings are that the main process parameters defining the mechanical properties of the deposited at low temperature Ti-Al-N coatings are: reactive gas flow rate, sputtering temperature and plasma cleaning time.

Keywords: physical vapour deposition (PVD), unbalanced magnetron sputtering, Ti–Al–N layers, hardness, adhesion

INTRODUCTION

Physical vapour deposition (PVD) processes are widely used for deposition of oxidation and corrosion resistant coatings on tools or machine components. The PVD transition metal nitrides such as Titanium Nitride (TiN) have been widely used as protective hard coatings to increase the lifetime and performance of cutting and forming tools [1-5]. However, the main drawback of TiN is its limited oxidation resistance (approximately 500^{o}C). Later on, a light metal element such as aluminium was incorporated into the TiN forming Titanium Aluminium Nitride (TiAlN) to overcome its shortcoming of instability at high temperatures. Furthermore, TiAlN coatings have been developed as an alternative to TiN, because of their higher oxidation resistance (approximately 750–800^{o}C), enhanced hardness (30–35 GPa) and higher corrosion resistance [6-11].

TiAlN films have been widely developed in many application fields such as cutting, forming tools, semiconductor devices, optical instruments, diffusion and biocompatible barriers [8-10]. A fundamental advantage of TiAlN films is that during heating they form a highly adhesive, dense protective Al_2O_3 film on the surface preventing further inward diffusion of oxygen into the coated material [11]. Among the many materials that can be chemically modulated in a multilayer, TiAlN is a favourite since it has a reputation for being wear resistant and chemically stable at high working temperatures.

Many studies have been reported on the deposition and properties of TiAlN coating produced by various techniques [12]. Among PVD coating technologies, reactive magnetron sputtering is a very useful method for producing different types of coatings including TiAlN. Although the basic sputtering process has been known and used for many years, the developed unbalanced magnetron and its incorporation into multi-source "closed-field" systems is responsible for the rise in importance of this technique. Closed-field unbalanced magnetron sputtering (CFUBMS) is an exceptionally versatile technique for the deposition of high-quality, well-adhered films. The main advantages of this technique are as follows: possibility for deposition at low temperatures, including room temperature; use of non-toxic working gases; a high degree of smoothness, uniformity and density of the deposited coatings. In order to improve the efficiency of coating process several modifications of magnetron sputtering techniques have been developed [13-19].

It is known that protective hard coatings (Ti, Al) N are generally deposited at temperatures of 400-500 ºC which provide high adhesion of the coating to the substrate, but lead to structural changes and

* To whom all correspondence should be sent:
ipfban-dve@mbox.digsys.bg

could worsen the substrate material properties. However, some instrumental materials such as carbon tool steel (U12) have low thermal resistance (≤200ºC) which requires low-temperature deposition of the coatings to protect the instruments from overheating. The requirement to maintain a low temperature during deposition of the Ti-Al-N coatings complicates the preparation process. Hence, the establishment of optimal technological regimes providing stable and high functional properties of the system "tool-coating" is necessary. This task could be solved by developing a multilayer coating since each sub-layer has defined composition, structure, optimal adhesion, physical-mechanical, tribological and corrosion resistance properties. Notwithstanding, the fact that TiAlN coatings have been used for many years, there are few articles on their preparation at low temperatures [18-20].

The results of the study of the physical and mechanical properties of TiAlN coatings deposited via CFUBMS process at the low temperatures are presented in this article.

EXPERIMENTAL DETAILS

The multilayer Ti-Al-N coatings were deposited in a temperature range of 150 - 200 ºC by reactive unbalanced magnetron sputtering (UDP 850-4, Teer Coatings Ltd.) from two titanium (99,99 %) and two aluminium (99,99%) rectangular targets in a closed-field configuration. The coatings were deposited onto two types of hardened substrates: high-speed steel (HSS) and carbon tool steel (U12). Prior to coating deposition, the substrates were cleaned in a special alkaline solution in an ultrasonic bath at 60 °C for 10 minutes to remove oils used for steel protection against corrosion, ten followed by a rinse in de-ionized water and drying at 140 °C. In general, after the cleaning procedure metal substrates contain an oxide layer which critically affects the adhesion of substrate-coating. Due to this, prior to the coating deposition, the substrates were cleaned in situ by ion etching in pure argon atmosphere under typical cleaning conditions: low magnetron power and a high negative pulsed DC bias potential on the substrate. Prior to the deposition, the vacuum chamber was evacuated to a base pressure of 2×10^{-3} Pa. After the evacuation, Ar or Ar + N_2 mixture was introduced into the chamber. The Ar flow rate was controlled by mass flow controller and the flow rate of the reactive gas N_2 was controlled by Optical Emission Monitor (OEM).

In the deposition process, the substrates were rotated biaxially at a speed of 5 rpm in order to obtain homogenous film thickness and composition, and the distance between the substrates and the targets was 150 mm. In Table 1. are summarized the basic parameters for the TiAlN coatings deposition.

Table 1. Experimental conditions for the TiAlN coatings deposition

Process	Parameter	Value
Chamber evacuation	Base pressure	2×10^{-3} Pa
Plasma cleaning	Negative substrate bias	500 V
	Ti target current	0.5 A
	Time	5 – 20 min
	Ar flow rate	25 sccm
Coating deposition	Substrate bias	-70 V
	Ti target current	5.0 A
	Al target current	0.3 - 3.0 A
	N_2 flow rate	0.5 - 16 sccm
	Substrate temperature	150 - 200°C
	Film thickness	1.2 - 1.6 μm

The deposition of the multilayer Ti-Al-N coatings starts with a Ti bond layer (~ 100 nm) followed by two TiN interlayers (graded and stoichiometric, ~ 250 nm), then the Al content is increased gradually to form a graded Ti-Al-N transition layer and the structure is then completed with a Ti-Al-N layer. Graded interfaces are routinely formed to ensure that stress induced in the coating is dissipated away from the coating-substrate interface. All the films were deposited at a bias voltage of -70V and a frequency of 150 kHz, in pulsed regime of the Al cathodes and DC regime of the Ti cathodes using a mixture of argon (99.9999%) and nitrogen (99.9999%) gases with different partial pressure ratio. The Ar flow rate was kept constant (25 sccm) in all of the experiments.

Measurements of the coating thickness were performed by a Calotest which is a suitable method for obtaining quick information about layer configuration, abrasion resistance and thickness. A stainless steel ball (~ 30 mm diameter) is used with diamond slurry with particles of 0.25 μm in diameter. The coating was abraded until the substrate was reached by the ball. After that, the coating was placed under an optical microscope where the circular crater shape was used to measure

the coating thickness by comparing the relative diameter of the exposed surface layers to the known diameter of the ball. The thickness was calculated using the CCD camera of the CPX Compact Platform of Anton Paar, CSM Instruments.

The mechanical properties of the deposited coatings were investigated using Compact Platform CPX (MHT/NHT) CSM Instruments equipment. Nanoindentation was performed by a triangular diamond Berkovich pyramid in the loading interval of 15 - 200 mN. The nanohardness and elastic modulus were determined by applying the Oliver & Phar method. The microscratch tests for coating adhesion and friction coefficient determination were performed using a spherical Rockwell indenter with a radius of 200 μm at normal force, progressively increasing from 1 N to 30 N.

Powder X-ray diffraction pattern of the sample was collected within the range from 5.3 to 80°2θ with a constant step 0.02°2θ and counting time 175 sec./step on Bruker D8 Advance diffractometer (Germany) with Cu Kα radiation and LynxEye detector. Diffraction patterns from the coating were obtained with a detector scan at fixed tube position with tube angle 10° and 5°. Phase identification was performed with the Diffracplus EVA using ICDD-PDF2 (2014) Database. The unit cell parameters and mean crystallite size were determined with the Topas-4.2 software package using the fundamental parameters peak shape description, including appropriate corrections for the instrumental broadening and difractometer geometry.

XPS studies were carried out in an ESCALAB MkII (VG Scientific) electron spectrometer with an Al K, (1486.6 eV) X-ray source. In order to obtain information about chemical composition of the Ti-Al-N coatings, XPS measurements were taken.

RESULTS AND DISCUSSION

Coating thickness

A series of multilayer TiAlN coatings were deposited on commercially available 5 mm thick HSS (EN: 1.3343) and carbon tool steel (EN:CT 120) substrates with diameter of 20 mm and 12 mm accordingly. Coating thickness measurements were taken by applying a Calotest method. The thickness of the deposited coating was calculated from measurements of the diameters of the craters in the coating and substrate. Fig.1 shows a segment of the optical microscopy image of the TiAlN coating architecture, obtained by ball-cratering test. This technique can be easily adapted for the measuring of the thickness of the different layers in a multilayered coating as long as the individual layers are easily distinguished and of sufficient thickness to be resolved by the microscope used to view and measure the crater diameters.

The calculated total thickness for all deposited coatings was in the range of 1.2 –1.6 μm.

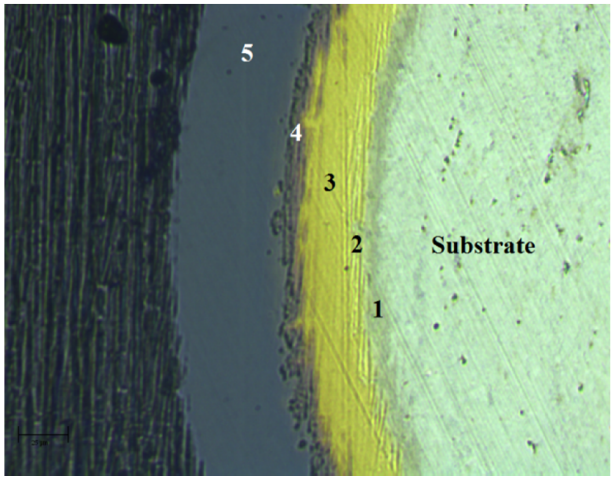

Fig.1. A segment of the optical microscopy image of the TiAlN coating architecture, obtained by ball-cratering test: (1)- Ti bond layer; (2)- TiN graded interlayer; (3)- TiN stoichiometric interlayer; (4)- TiAlN transition layer; (5)- TiAlN top layer

Mechanical properties

The mechanical properties of the multilayer TiAlN coatings obtained at different deposition conditions are summarized in Table 2. The hardness (H) and elastic modulus (E) were determined from the indentation loading/unloading curves generated with a Berkovich indenter using the Oliver–Pharr method [22]. A maximum load of 15 mN was applied, which corresponded to maximum indentation depths of less than 15% of the coating thickness, to minimize the substrate influence on the measurement. In our experiments, all the films were deposited at a constant bias voltage of -70 V and a frequency of 150 kHz in pulsed regime of the Al cathodes and DC regime of the Ti cathodes. The substrate bias plays an important role in determining the mechanical properties of the coatings. The use of ion bombardment allows deposition of adherent coatings at low substrate temperatures. In general, the hardness increases with the substrate bias up to 100 V, and does not change significantly at higher bias values [21]. Nanoindentation measurements reveal that the TiN interlayers (see Table 2) have nanohardness of 24 GPa and elastic modulus of 297 GPa. The measured mechanical properties lead to a H/E ratio of 0.08. The TiAlN coatings deposited at

substrate temperature of 200°C presented maximum hardness H= 38 GPa and elasticity modulus E = 418 GPa. However, this temperature is not recommended for deposition onto carbon tool steel U12 substrate due to its low thermal resistance (≥ 200 ºC). For this reason, the main deposition processes are developed at lower temperatures. The TiAlN coatings (Table 2) obtained at a temperature of 170 °C and nitrogen flow rate of 14.6 sccm possessed a good combination of mechanical properties- high coating hardness (26-31 GPa) and high adhesion to the substrate material (> 30 N). G.S. Kim et al. [19] reported similar hardness (38 GPa) for TiAlN coatings with the same chemical composition obtained by CFUBMS at temperature of deposition of 100ºC. Good hardness value (31 Gpa) were achieved by Z.-J. Liu et al. [20] where deposition was done at room temperature for nanocristalline TiAlN films with a content of Al (x=0.41). But in these publications, no information on the adhesion of coatings are provided.

Table 2. Results of mechanical properties characterization of the selected TiAlN coatings

Samples	Substrate temperature T [ºC]	Coating thickness [µm]	Hardness H [GPa]	Elastic modulus E [GPa]	Plasticity index H/E	OEM [%]	Cleaning time t [min]	COF µ	Critical load Lc [N]
TiN	170	1.0	24	297	0.08	60	10	0.11	> 30
TiAlN- #26	200	1.2	38	418	0.09	45	10	0.09	> 30
TiAlN- #71	150	1.2	28	392	0.071	45	10	0.1	19.3
TiAlN- #79	170	1.3	31	374	0.083	45	7	0.1	21.4
TiAlN- #81 HSS substr,	170	1.4	27	353	0.076	45	20	0.1	> 30
TiAlN- #81 U12 substr.	170	1.4	29	367	0.079	45	20	0.1	> 30
TiAlN- #97 HSS substr.	170	1.6	29	395	0.074	40	7	0.09	15.6
TiAlN- #97 U12 substr.	170	1.6	26	513	0.05	40	7	0.13	14.0

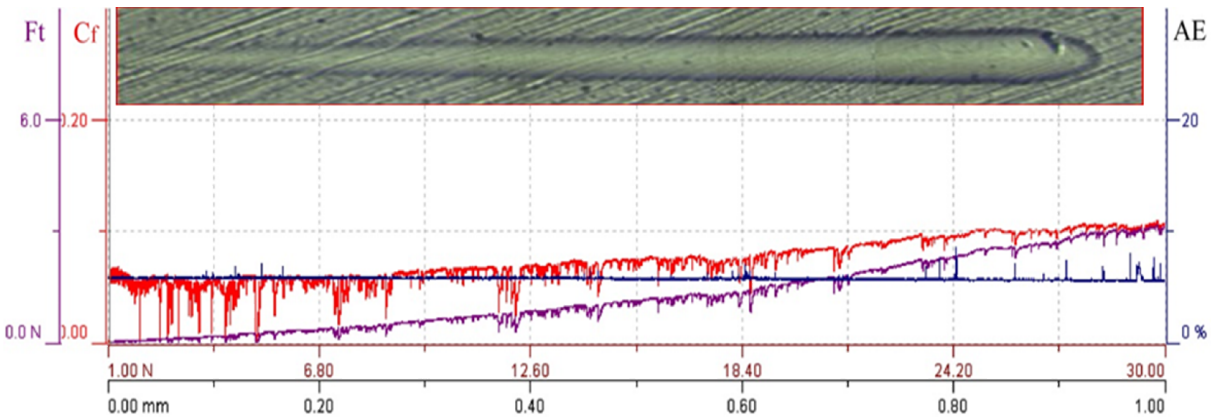

Fig.2. Optical micrograph of the scratch track in the TiAlN coating #81 and scratch test results of the acoustic emission (AE), friction force (Ft) and coefficient of friction (Cf)

The adhesion and toughness of the coatings were evaluated by a microscratch technique, using Rockwell diamond indenter with 200 µm tip radius. During the tests the load was progressively increased in linear mode from 1N to 30 N at scratch lengths of 1 mm and 3 mm at a constant scratching speed of 0.02 mm/min. The measurement device registered the friction force, friction coefficient, indenter penetration depth and acoustic emission along the scratch track. Three scratches for each sample were done. Critical loads were determined after the test by optical microscopy observation of the damages formed in the scratch tracks and from the recorded acoustic emission (AE) and friction

force (Ft) signals. The critical load values Lc1 and Lc2 indicate the loads when first cohesive and adhesive cracks appeared, respectively [18, 26].

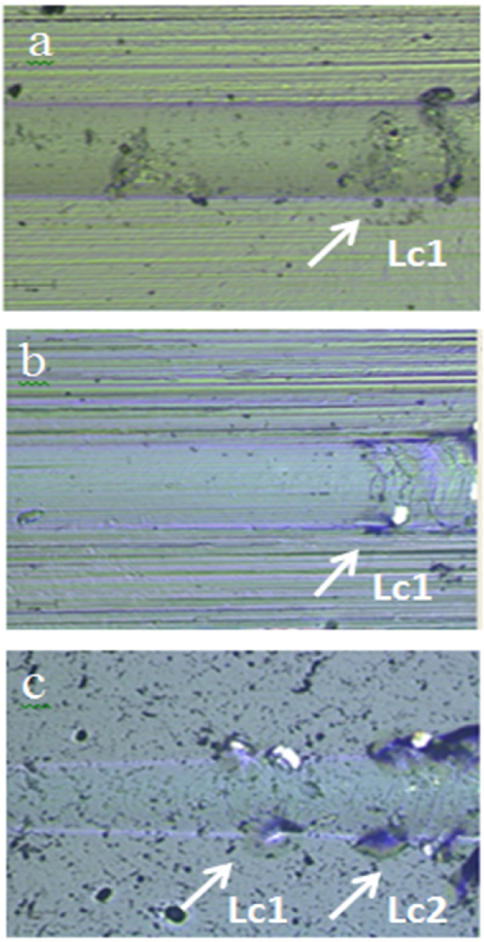

Fig.3. Main parts of scratch tracks with marked critical loads Lc1 and Lc2 in the TiAlN coatings: a) #71, b) #79 and c) #97 deposited at different deposition conditions

The critical loads corresponding to a load leading to the appearance of the first crack Lc1 for the selected coatings are presented in Table 2. It shows that the TiAlN coatings #26 and #81 have the best adhesion result without any visible damages within 30 N. An optical micrograph of the scratch track in the TiAlN coating #81 and scratch test results of the acoustic emission (AE), friction force (Ft) and coefficient of friction (Cf), are shown in Fig.2. As a result of the tests carried out, it was established that the critical load Lc1 for the coatings deposited at high N_2 flow rate (40% OEM) lies in the loading range 14 -16 N. presented The main parts of scratch tracks in the TiAlN coatings #71 (a), #79 (b) and #97 (c) are presented in Fig.3. The first symptoms of these coating damages (Lc1) are observed in the form of arch cracks (#71 and #79) and on scratch part of #97 there are small chippings on the scratch edges. Along with the load increase, semicircles are leading to a local delamination of the coating. In general, the coatings deposited on the HSS substrate show better adherence to the substrate than coatings deposited on the carbon tool steel U12 substrate. Y. Pinot et al. [18] reported properties of hard TiAlN coatings with different Al content ($0.46 \leq x \leq 0.62$) deposited at room temperature by r.f magnetron reactive sputtering from TiAl alloy targets. Contrary to our results, on these coatings lower adhesion strength was observed (Lc1 ≤ 8.5 N).

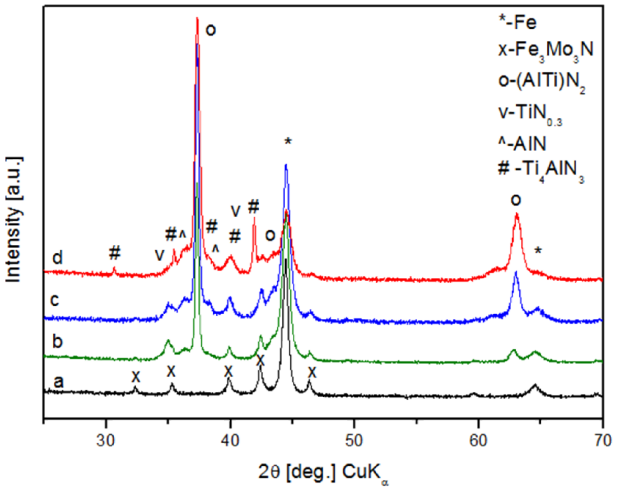

Fig.4. XRD patterns of a) substrate SS, b) substrate with coating at normal θ-2θ geometry, c) detector scan with fixed tube position at 10°, d) detector scan with fixed tube position at 5°

XRD analysis

The X-ray diffraction patterns of the coatings in the hard metal-coating system are difficult to obtain due to overlapping of the coating peaks with those of the substrate. With the aim to reduce the substrate effect, the grazing incidence X-ray diffraction method with a constant incident angles beam was used. The results from XRD analyses are summarized in Fig.4. Spectrum (a) shows the diffraction pattern of the SS-substrate, spectrum (b) represents the XRD pattern of the coating over the substrate in normal (θ-2θ) geometry while spectra (c) and (d) represent the diffraction patterns collected with a fixed tube position with angle 10° and 5° respectively (the signal is obtained predominantly from the coating). The HSS substrate is represented by two sets of peaks – the main phase corresponds to the cubic Fe phase. Due to the high values of molybdenum and tungsten presented in the steel, a second set of lines is also presented in the diffraction pattern of the substrate

corresponding to composition Fe_4W_2N and/or Fe_3Mo_3N (the peaks of these two phases overlap).

The coating itself comprises mainly the phase $(AlTi)N_2$ which crystallizes in the cubic Fm-3m space group with unit cell parameter a = 4.175 Å close to the value 4.172 Å given in ICDD PDF2 #71-5864. Mean crystallite size of the $(AlTi)N_2$ phase is 44 (1) nm. The presence of small peaks of some impurity phases as $TiN_{0.3}$, AlN and Ti_4AlN_3 could be seen as indication of some local inhomogeneity of the coating layer.

XPS analysis

Fig.5 represents the high resolution XPS spectra results of the multilayer TiAlN coating of #81 before and after the sputter etching. It is observed that the peak associated with Ti metal (Fig.5a) consists of two peaks centred at 457.0 eV and 462.1 eV. These peaks originate from Ti 2p3/2 and Ti 2p1/2 electrons in titanium oxynitride [25, 26]. Fig.5(b) shows the XPS spectra for the corresponding Al 2p levels of #81. The contribution in Fig.5(b) with maximum binding energy at 73.7 eV is assigned to Al-N chemical bonding state within the coating [27]. The fact that after etching the N1s spectrum shows only one peak with binding energies of approximately 396.3 eV (Fig.5c) is attributed to the presence of nitride films (TiN and AlN) [25].

The concentrations of titanium, aluminium and nitrogen in the coating top layer (#81) as determined by XPS analysis are 24,3 at.%, 33,4 at.% and 42,3 at.%, respectively. As expected, when the Al target current increases, the relative Al content in the film also increases during the transition Ti-Al-N layer deposition, while the reverse trend is seen for the Ti content.

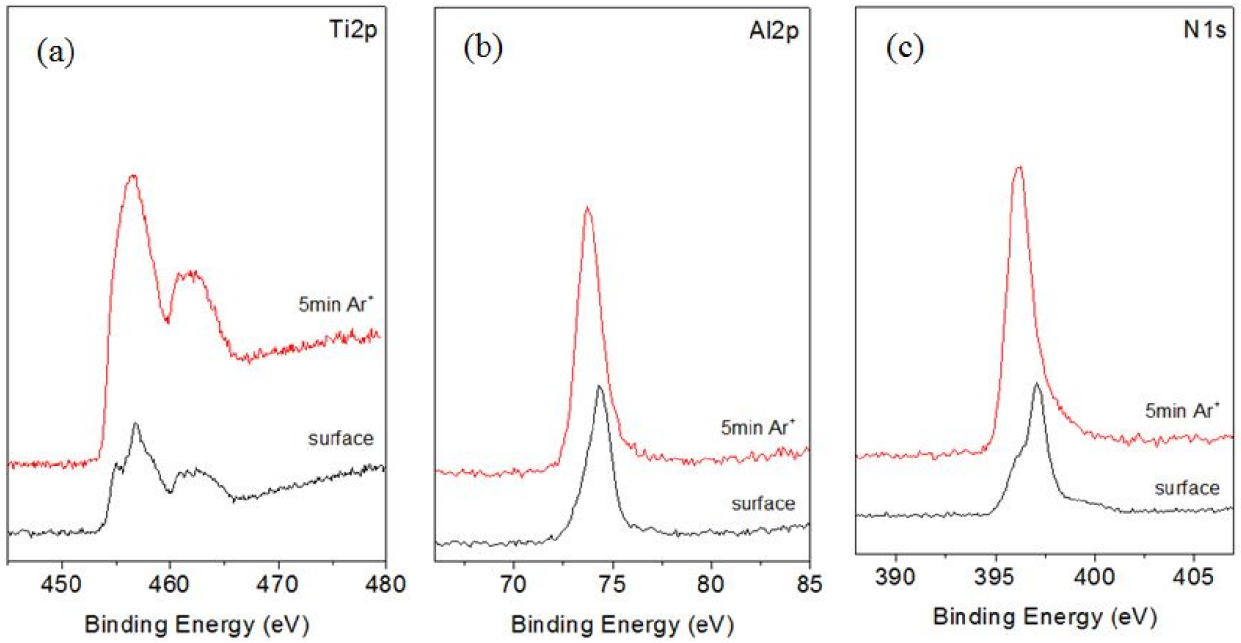

Fig.5. XPS spectra of (a)- Ti 2p, (b)- Al 2p and (c)- N 1s of the TiAlN sample (#81) before and after sputter etching in Ar^+ to remove the contaminated surface layer

The XPS results of the top layer show that the fraction (x) of Al atomic concentration [Al /(Ti + Al)] is approximately 0,58. This result is in line with the XRD results. The main AlTiN phase reveals the lattice constant to be approximately 4.17 Å which is significantly lower as compared to the reference value of 4.24 Å for pure TiN.

CONCLUSIONS

TiAlN coatings were prepared by closed-field reactive unbalanced magnetron sputtering on commercially available high speed steel and carbon tool steel with low thermal resistance. The coatings deposited at 200 ºC exhibit the greatest nanohardness and elastic modulus of 38 GPa and 418 GPa, respectively. Maximum value of the critical failure load (>30 N) was observed for the coating deposited at substrate temperature of 170ºC, nitrogen flow rate of 14,6 sccm and substrate cleaning time of 20 min. These coatings have very good adhesion strength. On the other hand, minimum critical failure load (Lc ≈15 N) was

observed for coatings deposited at substrate temperature of 170 ºC , nitrogen flow rate of 15,4 sccm and substrate cleaning time of 10 min. It can be concluded that the duration of plasma cleaning before deposition was mainly responsible for the adhesion strength of the coating to the substrate. The x-ray diffraction data shows formation mainly on the AlTiN phase with B1 NaCl structure and a mean crystallite size of 44 nm. The XPS analysis reveals that the coatings have $Ti_{0.42}Al_{0.58}N$ composition. It is evident, that the deposition of coatings with superior mechanical properties at low deposition temperatures needs to be controlled and balanced through careful selection of coating composition and development of processing conditions.

REFERENCES

1 Y.I. Chen, J.G. Duh, Surf. Coat. Technol., Vol. 46, Iss. 3, 371–384 (1991).
2 S. Yamamoto and H. Ichimura, J. Mater. Res., Vol. 11, No.5 (1996).
3 Ph. Roquiny, F. Bodart, G. Terwagne, Surf. Coat. Technol., 116–119, 278–283 (1999).
4 V. Chawla, R. Jayaganthan, R. Chandra, Mater. Charact., 59, 1015-1020 (2008).
5 N. Saoula, K. Henda et R. Kesrij, Plasma Fusion Res. SERIES, Vol. 8, 1403-1407 (2009).
6 Munz W D, J. Vac. Sci. Technol., 4, 2717 (1986).
7 J.C. Oliveira, A. Manaia, A. Cavaleiro, Thin Solid Films, 516, 5032 (2008).
8 C. Chokwatvikul, S. Larpkiattaworn, S. Surinphong, C. Busabok, P. Termsuksawad, Journal of Metals, Materials and Minerals, 21, 115 (2011).
9 D.G. Park, T.H. Cha, S.H. Lee, I.S. Yeo, J. Vac. Sci. Technol,. 19 (6), 2289 (2001).
10 J.T. Chen, J. Wang, F. Zhang, G.A. Zhang, X.Y. Fan, Z.G. Wu, P.X. Yan, J. Alloys Compd., 472, 91 (2009).
11 A. K. Singh, N. Kumari, S. K. Mukherjee, P. K. Barhai, IJRRAS., 14(3), 603 (2013).
12 S. PalDey, S.C. Deevi, Mater. Sci. Eng., A342, 58-79 (2003).
13 P.J. Kelly, R.D. Arnell, Vacuum, 56, 159-172 (2000).
14 J. Weichart, M. Lechthaler, IOP Conf. Series: Mater. Sci. Eng., 39, 012001 (2012).
15 S.K. Wu, H.C. Lin, P.L. Liu, Surf. Coat. Technol. 124, 97–103 (2000).
16 Q. Yang, D.Y. Seo, L.R. Zhao, X.T. Zeng, Surf. Coat. Technol. 188–189, 168–173 (2004).
17 A. Z. Ait-Djafer, N. Saoula, H. Aknouche, B. Guedouar, N. Madaoui, Appl. Surf. Sci., 350, 6–9 (2015).
18 Y. Pinot, M.-J. Pac, P. Henry, C. Rousselot, Ya.I. Odarchenko, D.A. Ivanov, C. Ulhaq-Bouillet, O. Ersen, M.-H. Tuilier, Thin Solid Films, 577, 74–81 (2015).
19 G.S. Kim, S. Lee, J. Hagh, Surf. Coat. Technol., 193, 213– 218 (2005).
20 Z.-J. Liu, P.W. Shum, Y.G. Shen, Thin Solid Films, 468, 161–166 (2004).
21 21. H. C. Barshilia, N. Selvakumar, K.S. Rajam, A. Biswas, Sol. Energy Mater. Sol. Cells, 92, 1425–1433 (2008).
22 22.W.C. Oliver, G.M. Pharr, J. Mater. Res., Vol. 19, No.1, 3-20 (2004).
23 23.L. García-González, M. G. Garnica-Romo, J. Hernández-Torres and F. J. Espinoza-Beltrán, Braz. J. Chem. Eng., Vol. 24, No. 02, 249 – 257, (2007).
24 24.T.Weirather, K. Chladil, B. Sartory, D. Caliskanoglu, R. Cremer, W. Kölker, C. Mitterer, Surf. Coat. Technol., 257, 48–57 (2014).
25 25.H. C. Barshilia, K. Yogesh, K.S. Rajam, Vacuum, 83, 427–434 (2009).
26 26.P.W. Shum, Z.F. Zhou, K.Y. Li, Y.G. Shen, Mater. Sci. Eng., B100, 204–213 (2003).
27 27.Yi , L. Peng , J. Huang, Mater. Sci. Eng., C59, 669–676 (2016).